Histol Histopathol (2021) 36: 229-237

**http://www.hh.um.es**

Histology and Histopathology
*From Cell Biology to Tissue Engineering*

**ORIGINAL ARTICLE** **Open Access**

# Silencing of SETD6 inhibits the tumorigenesis of oral squamous cell carcinoma by inhibiting methylation of PAK4 and RelA

**Wentao Huang[1], Hongjing Liu[2] and Tianzhu Lv[2]**

[1]Savaid Stomatology School, Hangzhou Medical College, Hangzhou, Zhejiang and

[2]College of Stomatology of Guizhou Medical University, Guizhou Medical University, Guiyang, Guizhou, China

**Summary.** Background. Oral squamous cell carcinoma (OSCC) is one of the most comment types of oral malignancies. SET-domain-containing protein 6 (SETD6) was recently identified as an important regulator of multiple signaling pathways through methylating protein substrates. Meanwhile, SETD6 is known to participate in multiple cancers. However, the role of SETD6 in OSCC remains unclear.

Methods. Gene and protein expressions in OSCC cells or tissues were detected by RT-qPCR and western blot, respectively. In addition, CCK-8 assay was used to test the cell viability. A transwell assay was performed to measure cell migration and invasion. Flow cytometry was used to test cell apoptosis and cycle. Meanwhile, methylation-specific PCR (MSP) was used to detect the status of promoter methylation.

Results. SETD6 was significantly upregulated in OSCC tissues. In addition, knockdown of SETD6 notably inhibited the proliferation and induced the apoptosis of OSCC cells. Furthermore, silencing of SETD6 notably suppressed the migration and invasion of OSCC cells. Meanwhile, SETD6 siRNA significantly inhibited the promoter methylation of RelA (NF-κB p65) and PAK4. Furthermore, SETD6 siRNA induced G1 arrest in OSCC cells.

Conclusion. Knockdown of SETD6 inhibits the tumorigenesis of OSCC by suppressing promoter methylation of PAK4 and RelA. Therefore, our study might shed new light on exploring strategies for the treatment of OSCC.

**Key words:** OSCC, SETD6, NF-κB, Methylation

*Corresponding Author:* Tianzhu Lv, College of Stomatology of Guizhou Medical University, Guizhou Medical Unviersity, 481 binwen Road, Hangzhou, Zhejiang 310053, China. e-mail: ltz_0628@126.com

DOI: 10.14670/HH-18-327

## Introduction

Oral squamous cell carcinoma (OSCC) is one of the most aggressive cancers with high malignant behaviors (Nakamichi et al., 2021). Moreover, the incidence of OSCC is nearly 300,000 new cases all over the world every year (Sowmya et al., 2020). Betel quid, smoking and HPV infection are known to be the major risk factors which lead to OSCC (Gilligan et al., 2020; Jayaraj et al., 2020; Oliveira Alves et al., 2020). Furthermore, OSCC is known as a propensity for metastasis (Bai et al., 2020). At present, surgery, chemotherapy and radiotherapy are the major methods of the treatment of OSCC (Wong et al., 2020). However, the effect remains not ideal (Chen et al., 2021). Great efforts have been made to study OSCC. For example, Zhang et al. found that Forkhead promotes EMT and chemoresistance by upregulating lncRNA CYTOR in OSCC (Zhang et al., 2021); Zhou et al. revealed that Akt signaling played an important role in tumorigenesis of OSCC (Zhou et al., 2021). However, more studies are needed to explore the pathogenesis of OSCC.

The SET-domain-containing protein 6 (SETD6) is a member of the protein lysine methyltransferases (PKMTs) family, and it is known as a lysine methyltransferase (Dai et al., 2020). In addition, SETD6 is linked to the tumorigenesis of multiple cancers. For instance, upregulation of SETD6 could inhibit the progression of gastric cancer (Bai et al., 2019); Yao et al. indicated that SETD6 might promote breast cancer cell proliferation and migration (Yao et al., 2018). However, the function of SETD6 in OSCC remains unclear.

P65 (RelA) is known to be a crucial mediator during immune and inflammatory responses (Levkau et al., 1999). P21-activated kinase 4 (PAK4) is a member of the serine/threonine kinases family is over-expressed in numerous cancer tumors and is associated with oncogenic cell proliferation, migration and invasion (Vershinin et al., 2020). SETD6 might methylate RelA at

Lysine 310, thus inhibiting the activation of NF-κB target genes (Walter et al., 2020). In addition, it has been reported that SETD6 might regulate the WNT signaling pathway by methylation of PAK4 at Lysine 473 (Vershinin et al., 2016). However, the correlation between SETD6 and RelA (or PAK4) in OSCC is not clear. In the current study, we sought to investigate the function of SETD6 in OSCC. We hope this research will shed new light on exploring new strategies for the treatment of OSCC.

## Materials and methods

### *Cell culture and cell transfection*

OSCC cell lines (Cal-27 and SCC-9) and normal oral cells (HOK) were obtained from American Type Culture Collection (ATCC, Rockville, MD, USA). Cells were maintained in Dulbecco's Modified Eagle's medium (DMEM, Thermo Fisher Scientific, Waltham, MA, USA), supplemented with 10% fetal bovine serum (FBS, Thermo Fisher Scientific), 100 U/ml penicillin and 100 $\mu$g/ml of streptomycin in a humidified incubator with 5% $CO_2$ at 37°C. siRNAs targeted against SETD6 (SETD6 siRNA1, SETD6 siRNA2 and SETD6 siRNA3; 10 nM) and a negative control siRNA (siRNA-NC) were purchased from Guangzhou RiboBio Co., Ltd. and transfected into OSCC cells ($5x10^3$) using Lipofectamine® 2000 (Thermo Fisher Scientific, Inc.), according to the manufacturer's instructions. Cells were incubated at 37°C for 6 h before subsequent experiments were performed. Transfection efficiency was determined using reverse transcription-quantitative PCR (RT-qPCR). The sequences of the siRNAs were as follows: Negative control siRNA, 5'-UUCUCCGAACGUGUCACGUTT-3'; SETD6 siRNA1, 5'-GGAAUGAAGCAACUGA GAUUU-3'; SETD6 siRNA2, 5'-GGGTTACGATTGCC CAGAT-3' and SETD6 siRNA3, 5'-CGTTAAGGTTCC GGACGAC-3'.

### *Tissue collection*

In total, 30 pairs of OSCC samples and adjacent normal tissues were collected from the Affiliated Stomatological Hospital of Guizhou Medical University between August 2018 and August 2019. The clinical and pathological data of these patients were collected with their written informed consent. The expression of SETD6 in OSCC and adjacent normal tissues was detected by immunohistochemistry (IHC) staining as previously described (Ferrari et al., 2020).

### *The Cancer Genome Atlas (TCGA)*

The expression of SETD6 in OSCC tissues or adjacent normal tissues was analyzed by TCGA. The data of TCGA were analyzed from Gene Expression Profiling Interactive Analysis (GEPIA) as previously described (Tang et al., 2017).

### *IHC staining*

Tissues of patients were fixed in 4% paraformaldehyde in PBS overnight, paraffin-embedded, and cut into 5 μm-thick sections. Paraffin sections were deparaffinized and rehydrated. The sections were heated in sodium citrate buffer in a microwave for antigen retrieval, washed with phosphate-buffered saline (PBS) for 5 min (three times) at room temperature, incubated in 3% $H_2O_2$ at room temperature for 25 min. The sections were washed with PBS for 5 min (three times) and blocked and incubated in goat serum for 30 min. Then, the samples were stained with primary antibodies (anti-SETD6) overnight at 4°C. After that, samples were incubated with secondary antibody (HRP-labeled) for 30 min at 37°C. Finally, freshly prepared diaminobenzidine (DAB) was added for color development. All the antibodies were obtained from Abcam (Cambridge, MA, USA). The tissues were observed under a fluorescence microscope.

### *Real-time reverse transcriptase quantitative PCR (RT-qPCR)*

Total RNA was extracted from OSCC cells using TRIzol reagent (Takara, Inc.). Subsequently, cDNA was synthesized using PrimeScript RT reagent kit (ELK Biotechnology, Wuhan, China) according to the manufacturer's instructions. The temperature and duration of RT were as follows: 37°C for 60 min and 85°C for 5 min. The RT-qPCR was performed by the SYBR® Premix Ex Taq™ II kit (ELK Biotechnology) on a 7900HT system (Applied Biosystems, CA, USA) according to the following conditions: Initial denaturation for 10 min at 95°C; 40 cycles of 95°C for 15 sec and 60°C for 30 sec; and final extension for 1 min at 60°C. The primers used were as follows: RelA: (forward), 5'-CGCTTCGGCAGCACATATAC-3'; (reverse), 5'-AAATATGGAACGCTTCACGA-3'. PAK4: (forward), 5'-TCCCCCTGAGCCATTGTG-3'; (reverse), 5'-ACCTGTCTCCCCATCCA-3'. SETD6: (forward), 5'-GGTCCACGGCACGTTAACA-3'; (reverse), 5'-CCAATTGAAGGCCTTAAGG-3' and β-actin: (forward): 5'-TGCGCTAGCAGCGGGAAC AGTTC-3'; (reverse): 5'-CCAGTGCAGGGTCCGAG GTATT-3'. The relative level was normalized to β-actin using the $2^{-\Delta\Delta Ct}$ method.

### *Cell counting Kit-8 (CCK-8) assay*

Cell counting kit-8 (Beyotime, Shanghai, China) was applied to determine the cell viability according to the manufacturer's protocol. Cal-27 or SCC-9 cells were plated onto a 96-well plate at the density of $5.0\times10^3$ cells/well and incubated at 37°C overnight. After that, cells were transfected with siRNA-ctrl (NC), SETD6 siRNA1, SETD6 siRNA2 or SETD6 siRNA3 for 0, 24, 48 or 72h. Later on, 10 μL CCK-8 reagents were added into each well, and then cells were incubated for 2h at

37°C. The absorbance was detected at 450 nm using a microplate reader (Bio-Rad, Hercules, CA, USA).

### Transwell assays

For the cell migration assay, $2\times10^5$ OSCC cells were seeded into the upper chambers of the 24-well plates in 200 μL of serum-free RPMI 1640 medium supplemented with 0.2% bovine serum albumin. The lower chambers contained RPMI 1640 medium supplemented with 1% FBS. After 24h of incubation at 37°C, the non-migrating cells were gently removed from the upper side of each chamber with a cotton swab, while the cells that had migrated were fixed with 95% alcohol for 10 min and stained with 0.5% crystal violet (Sigma, Grand Island, NY, USA) for 5 min. Finally, cells were counted under an inverted light microscope (Olympus) at 400x magnification.

For the invasion assay, the upper chambers of the 24-well plates were pretreated with 50 μL of Matrigel (12.5 mg/L, (BD Biosciences, Franklin Lake, NJ, USA). Then, OSCC cells ($1\times10^6$ cells/ml) in FBS-free medium were seeded into the upper chambers. The lower chambers contained RPMI 1640 medium supplemented with 1% FBS. The cells were incubated at 37°C for 24h, and cells that had attached to the underside of the membrane were fixed and stained with 0.5% crystal violet solution. Finally, the number of invading cells was counted under a microscope at 400x magnification.

### Flow cytometry assay

The early and late apoptosis (Annexin-$V^+$ $PI^-$ plus Annexin-$V^+$ $PI^+$) of OSCC cells were measured by flow cytometry. OSCC cells were seeded into 6-well plates at a density of $1x10^6$ cells/well. Then, OSCC cells were collected and then resuspended in 100 $\mu$L binding buffer following centrifugation (4°C) at 500xg for 5 min. After that, the cell suspension was stained with 5 $\mu$l annexin V-FITC (BD Biosciences, Franklin Lake, NJ, USA) and 5 $\mu$l propidium iodide (PI, BD Biosciences) for 15 min. Later on, the cell apoptosis rate was measured using a flow cytometer (BD Biosciences) and the results were analyzed using FACS (BD Biosciences) with FlowJo (v10.6.2; FlowJo LLC).

### Western blot

Total proteins were isolated from OSCC cells using a RIPA buffer (Beyotime, Shanghai, China) and quantified with a BCA protein assay kit (Beyotime). Equal amounts of protein (30 μg) were separated by 10% SDS-PAGE, and then transferred onto polyvinylidene difluoride membrane (PVDF, Thermo Fisher Scientific). Non-fat milk (5%) in TBST was used to block the PVDF membrane at room temperature for 1h. Later on, PVDF membrane was incubated at 4°C overnight with the following primary antibodies: anti-SETD6 (1:1000, Abcam Cambridge, MA, USA), anti-Cyclin D1 (1:1000, Abcam), anti-PAK4 (1:1000, Abcam), anti-β-catenin (1:1000, Abcam), anti-c-Myc (1:1000, Abcam), anti-RelA (1:1000, Abcam), anti-p21 (1:1000, Abcam), anti-CDK4 (1:1000, Abcam), anti-Bcl-2 (1:1000, Abcam), anti-Active caspase 3 (1:1000, Abcam) and anti-β-actin (1:1000, Abcam). Then, the membrane was incubated with HRP-labeled goat anti-rabbit secondary antibody (1:5000, Abcam) for 1h at room temperature. Enhanced chemi-luminescence (ECL) reagent (Thermo Fisher Scientific) was used to visualize the protein bands according to the manufacturer's protocol. Image J Software was used to quantify the intensity of the bands. β-actin was used as an internal control.

### Methylation-specific PCR (MSP)

For MSP detection, a pair of primers to amplify only methylated CpG targets were obtained based on the CpG island sequence of the RelA/PAK4 promoter-proximal elements, and the sequences were as follows: RelA: 5'-TTATTTGTGGTAGAATTTTGGCG-3' (forward) and 5'-CATATTAATCCCAATACATACGTCG-3' (reverse); PAK4: 5'-CCAAATCGCTAGTGAUUUUCCCC-3' (forward) and 5'-AATTUUGGCCCACCCCGGG-3' (reverse). Another sequence of primers (performed to amplify unmethylated CpG targets) was as follows: RelA: 5'-ATTTGGCCCCGGACATTCCCCCAA-3' (forward) and 5'-GGCAACCTTGUUUCACCATC AGCAGCG-3' (reverse). MSP was performed with a standard PCR machine. The amplified DNA fragments were then subjected to 2% agarose gel electrophoresis.

### Cell cycle detection

Briefly, OSCC cells were harvested by accutase treatment and counted with a hemocytometer. $5\times10^5$ cells were fixed, permeabilized, and stained with PI (BD bioscience) in accordance with the manufacturers' instructions. Cells were analyzed by flow cytometry using a FACSCalibur measuring FL2 area versus total counts. The data were analyzed using ModFit (http://mycyte.org/) and FlowJo (http://mycyte.org/) software to generate the percentages of cells in G1, S, and G2 to M phases of the cell cycle as previously described (Zhang et al., 2018).

### Statistical analysis

All experiments were expressed as mean ± standard error (S.D.). CCK-8 assay was performed in quintuplicate. Cell transfection, RT-qPCR, IHC staining, flow cytometry, western blot, transwell migration and invasion assays were repeated triply. Graphs were generated using GraphPad Prism software (version 7.0, La Jolla, CA, USA). One-way analysis of variance (ANOVA) and Tukey's tests were performed for

comparisons between multiple groups. P value <0.05 was considered as statistically significant.

## Results

### *Knockdown of SETD6 significantly inhibited the proliferation of OSCC cells*

To detect the expression of SETD6, the Cancer Genome Atlas (TCGA) was used. As indicated in Fig. 1A, the expression of SETD6 in OSCC tissues was higher than that in adjacent normal tissues. Consistently, the protein level of SETD6 in OSCC tissues was significantly higher than that in normal tissues (Fig. 1B). Consistently, the level of SETD6 in OSCC cells was notably upregulated, compared with that in HOK cells (Fig. 1C). Meanwhile, the expression of SETD6 in OSCC cells was notably decreased by SETD6 siRNA (Fig. 1D,E). Moreover, OSCC cells were more sensitive to SETD6 siRNA2 or siRNA3, compared to siRNA1. Thus, SETD6 siRNA2 and siRNA3 were selected for use in subsequent experiments. Furthermore, silencing of SETD6 significantly decreased viability of OSCC cells (Fig. 1E,F). Taken together, knockdown of SETD6 significantly inhibited the proliferation of OSCC cells.

### *Silencing of SETD6 notably induced apoptosis and inhibited metastasis in OSCC cells*

In order to test cell apoptosis, flow cytometry was performed. As we expected, knockdown of SETD6 notably induced apoptosis of OSCC cells (Fig. 2A,B). Moreover, Cell migration and invasion of OSCC were obviously inhibited by SETD6 siRNA (Fig. 2C-F). Altogether, silencing of SETD6 notably induced apoptosis and inhibited metastasis in OSCC cells. Moreover, based on these data, OSCC cells were more sensitive to SETD6 siRNA3 than SETD6 siRNA2. Therefore, SETD6 siRNA3 was selected for further analysis.

### *Knockdown of SETD6 inhibited the methylation of PAK4 promoter*

For the purpose of investigating the correlation between SETD6 and PAK4, MSP was used. As shown in Fig. 3A, silencing of SETD6 notably inhibited the methylation of PAK4 promoter. In addition, the expression of PAK4 in OSCC cells was notably upregulated in the presence of SETD6 knockdown (Fig. 3B). Meanwhile, the level of PAK4 was notably downregulated in Cal-27 cells, compared with that in HOK cells (Fig. 3C). Moreover, silencing of SETD6

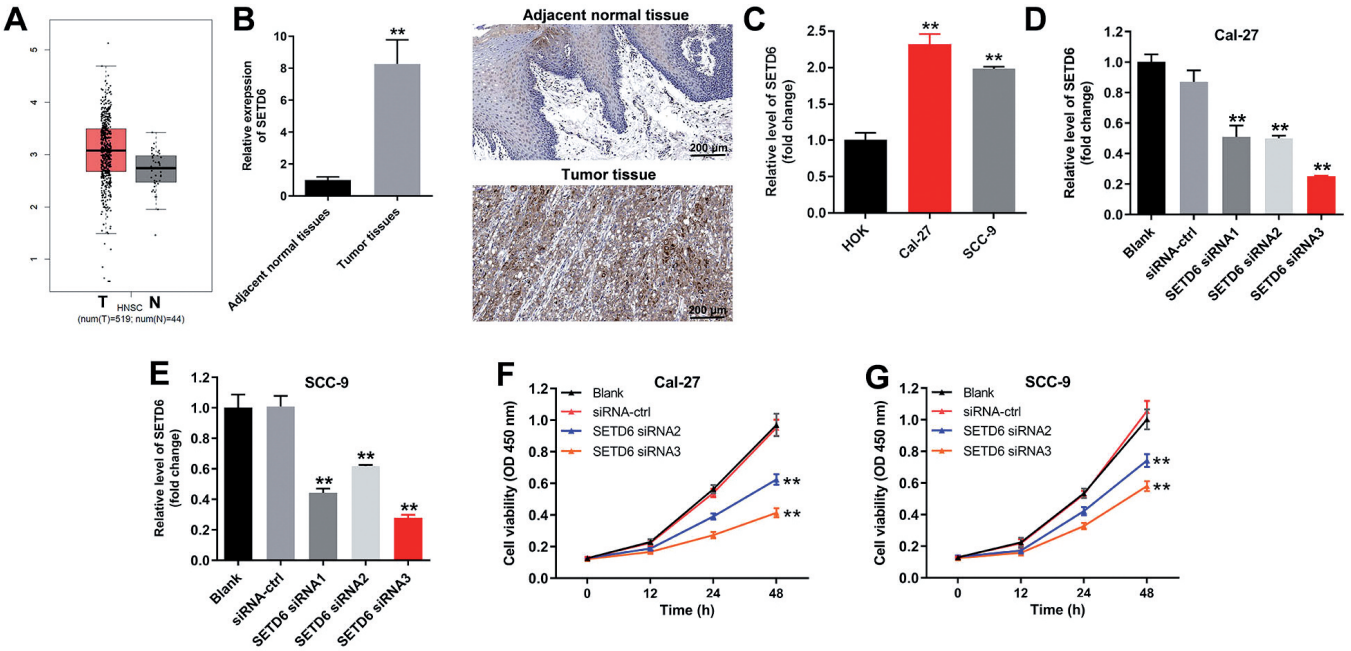


**Fig. 1.** Knockdown of SETD6 significantly inhibited the proliferation of OSCC cells. **A.** The expressions of SETD6 in OSCC and adjacent normal tissues were presented. The data were acquired from TCGA. **B.** The expressions of SETD6 in OSCC and adjacent normal tissues were detected by IHC staining. **C, D.** Cal-27 or SCC-9 cells were transfected with NC, SETD6 siRNA1, SETD6 siRNA2 or SETD6 siRNA3 for 24 h. Then, the expression of SETD6 in OSCC cells was detected by RT-qPCR. **E, F.** Cal-27 or SCC-9 cells were treated with NC, SETD6 siRNA2 or SETD6 siRNA3 for 0, 24, 48 or 72h, respectively. Then, the OD value of OSCC cells was tested by CCK-8 assay. **P<0.01 compared to control.

obviously inhibited the expressions of SETD6, β-catenin, cyclin D1 and c-Myc and upregulated the protein level of PAK4 in OSCC cells (Fig. 3D,E). To sum up, knockdown of SETD6 was able to inhibit the methylation of PAK4 promoter.

### *Silencing of SETD6 notably decreased the level of RelA (p65) promoter methylation*

To explore the correlation between SETD6 and RelA, MSP was used. As revealed in Fig. 4A, the state of RelA promoter methylation was significantly inhibited by SETD6 siRNA, and the expression of RelA in OSCC cells was notably upregulated by silencing of SETD6 (Fig. 4B). Meanwhile, the level of RelA was significantly upregulated in OSCC cells, compared with that in HOK cells (Fig. 4C). In addition, the expressions of RelA, p21 and active caspase 3 in OSCC cells were notably increased by SETD6 siRNA (Fig. 4D,E). In contrast, silencing of SETD6 significantly inhibited the levels of CDK4 and Bcl-2 in OSCC cells (Fig. 4D,E). Altogether, silencing of SETD6 inhibited the methylation of RelA (p65) promoter.

### *Knockdown of SETD6 notably induced G1 arrest in OSCC cells*

To test the cell cycle distribution, flow cytometry was used. As we expected, SETD6 siRNA significantly induced G1 arrest in OSCC cells (Fig. 5A,B). Therefore,

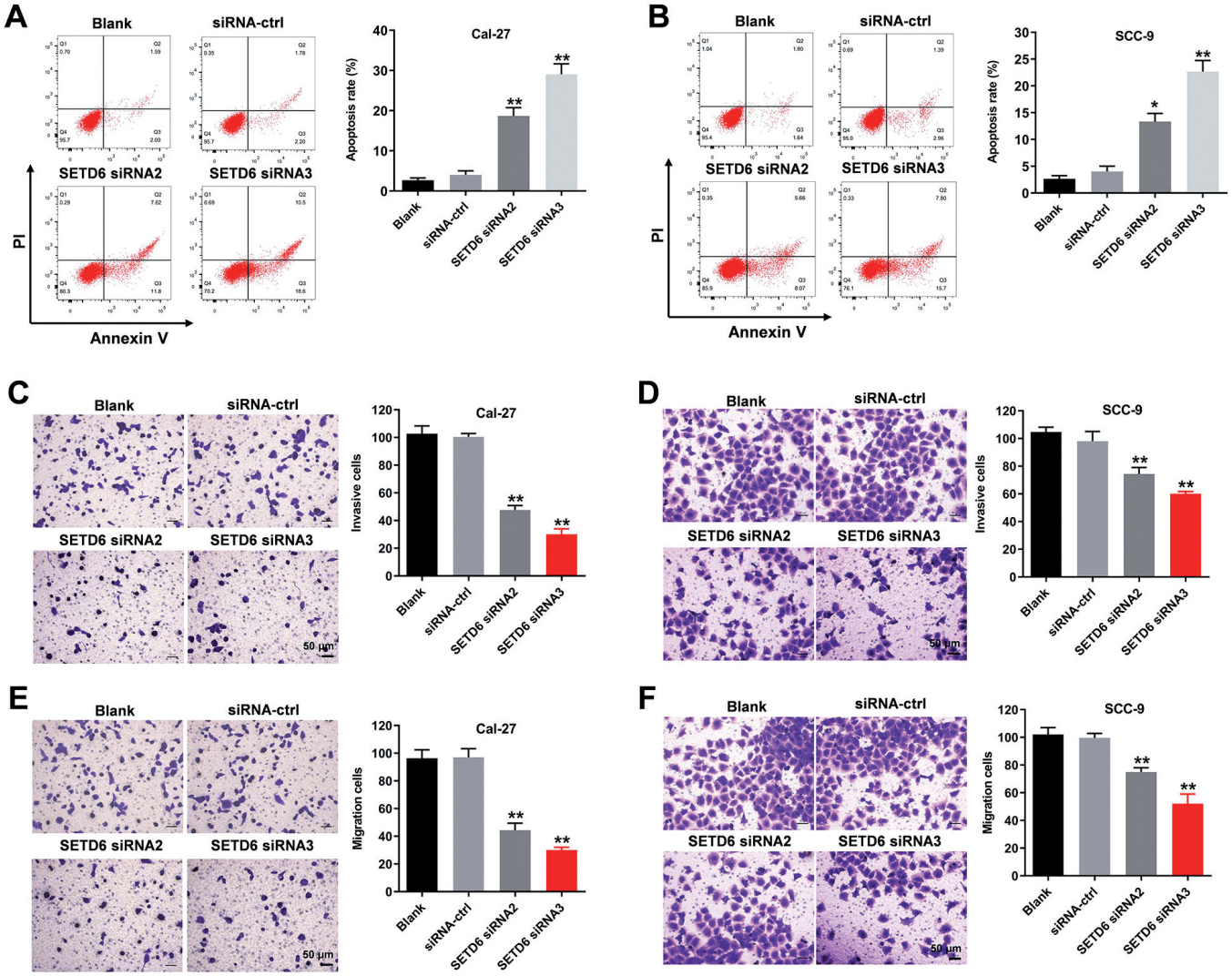


**Fig. 2.** Silencing of SETD6 notably induced apoptosis and inhibited metastasis of OSCC cells. **A, B.** The rate of apoptotic Cal-27 or SCC-9 cells was detected by FACS after double staining with Annexin V and PI. X axis: the level of Annexin-V FITC fluorescence; Y axis: the PI fluorescence. **C, D.** The invasion of Cal-27 or SCC-9 cells was tested using transwell invasion assay. *P<0.05, **P<0.01 compared to control. × 400.

knockdown of SETD6 inhibited the growth of OSCC cells by inducing G1 arrest.

## Discussion

It has been reported that SETD6 is involved in multiple cancers (Martin-Morales et al., 2017; Yao et al., 2018; Zhang et al., 2019). In this study, we found that SETD6 was upregulated in OSCC. This finding supplemented the role of SETD6 in OSCC. In addition, our finding firstly found SETD6 knockdown was able to inhibit the tumorigenesis of OSCC, suggesting that SETD6 might function as a key mediator in OSCC.

As we know, SETD6 might methylate PAK4 at Lysine 473 via binding to PAK4 (Vershinin et al., 2016). In addition, SETD6 might activate Wnt signaling by regulating the methylation of PAK4 (Vershinin et al., 2016). Consistently, our research indicated that silencing of SETD6 might inhibit the tumorigenesis of OSCC via inactivation of Wnt signaling. On the other hand, our findings suggested that SETD6 siRNA significantly inhibited the expression of c-Myc, CDK4 and Cyclin D1. These data further confirmed that SETD6 knockdown was able to inactivate Wnt signaling in OSCC.

It has been previously confirmed that SETD6 negatively regulated the activity of RelA (p65) (Vershinin et al., 2016). In addition, RelA is known to act as a scaffold for subsequent recruitment which leads to a constitutive cell growth inhibition and inflammatory responses (Levy et al., 2011; Maggirwar et al., 2000). Walter CEJ et al found that SETD6 might regulate NF-κB signaling in bladder cancer (Walter et al., 2020). Consistently, our data revealed that knockdown of SETD6 might inhibit the tumorigenesis of OSCC via upregulation of RelA. Meanwhile, SETD6 siRNA

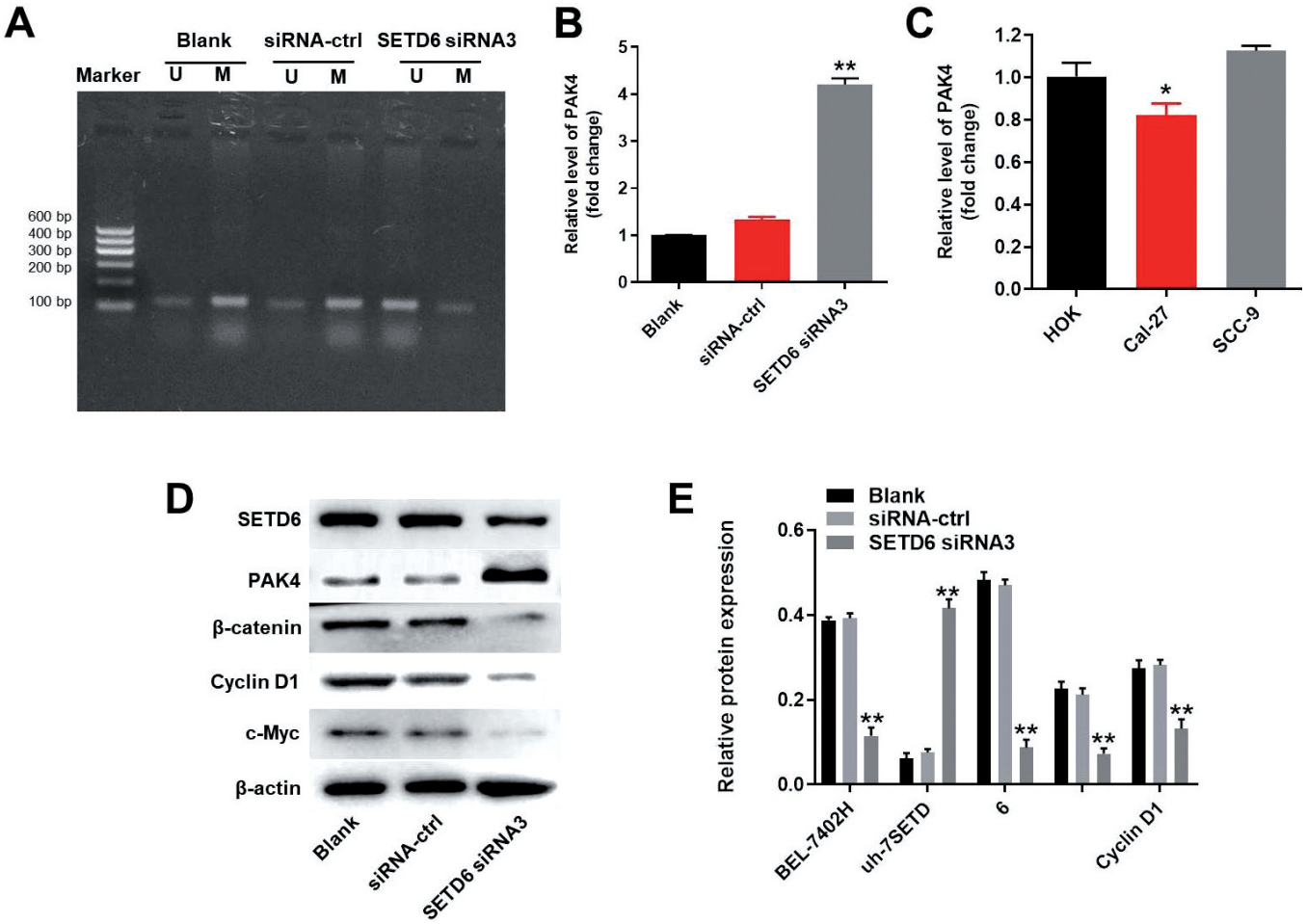


**Fig. 3.** Knockdown of SETD6 inhibited the methylation of PAK4 promoter. **A.** MSP of the PAK4 CpG island in OSCC cells treated with NC or SETD6 siRNA3. 'U' indicates unmethylated nucleotides. 'M' indicates methylated nucleotides. **B.** The expression of PAK4 in OSCC cells was detected by RT-qPCR. **C.** The expression of PAK4 in OSCC cells or HOK cells was detected by RT-qPCR. **D.** The protein expressions of SETD6, PAK4, β-catenin, Cyclin D1 and c-Myc in OSCC cells were detected by western blot. **E.** The relative expressions were quantified by normalizing to β-actin. **P<0.01 compared to control.

inhibited the expression of Bcl-2. A recent report indicated that SETD6 might upregulate MDM2 by methylating ReIA (Mukherjee et al., 2017), and MDM2 can positively regulate Bcl-2 (Liu et al., 2020). Therefore, it might be concluded that SETD6 siRNA inhibited the expression of Bcl-2 by inhibiting the

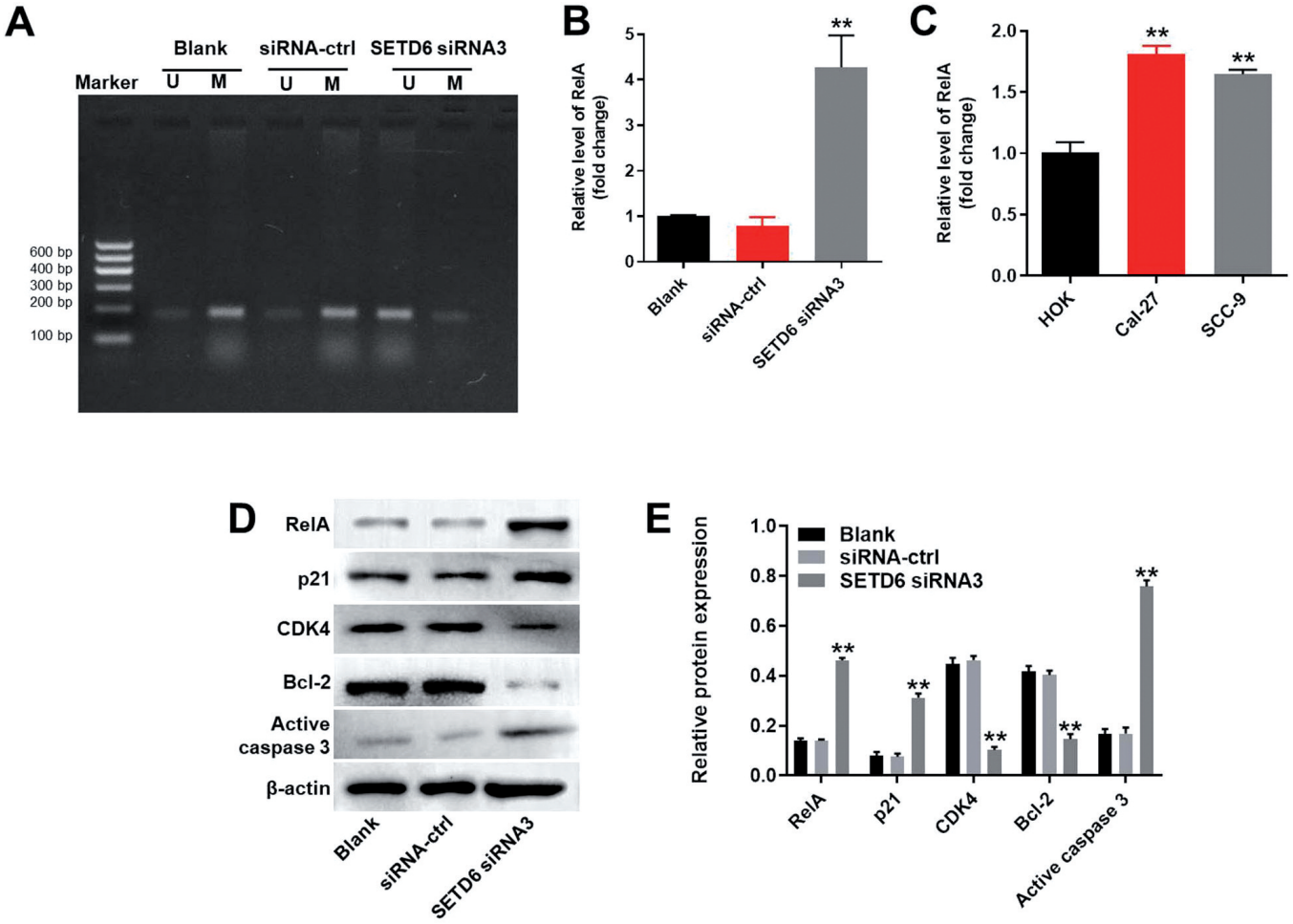


**Fig. 4.** Silencing of SETD6 notably decreased the level of RelA (p65) promoter methylation. **A.** MSP of the RelA CpG island in OSCC cells treated with NC or SETD6 siRNA3. 'U' indicates unmethylated nucleotides. 'M' indicates methylated nucleotides. **B.** The expression of RelA in OSCC cells was detected by RT-qPCR. **C.** The level of RelA in OSCC cells or HOK cells was investigated by RT-qPCR. **D.** The protein expressions of RelA, p21, Active caspase 3, CDK4 and Bcl-2 in OSCC cells were detected by western blot. **E.** The relative expressions were quantified by normalizing to β-actin. **P<0.01 compared to control.

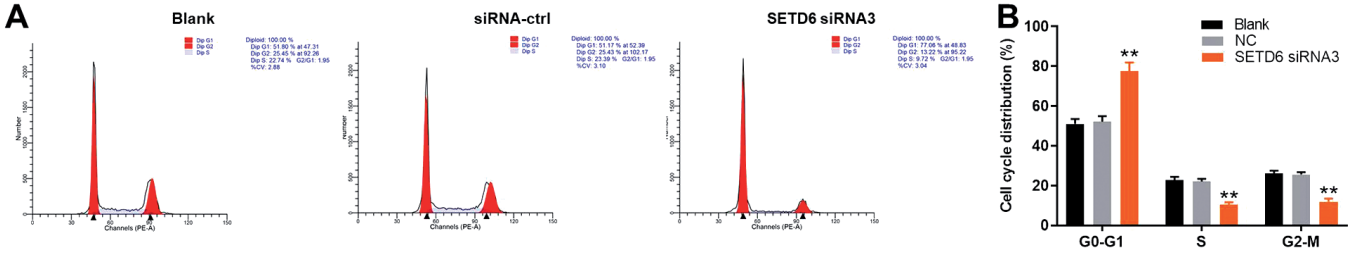


**Fig. 5.** Knockdown of SETD6 notably induced G1 arrest in OSCC cells. **A, B.** the cell cycle distribution in G0/G1, S, and G2 phase after propidium iodide staining of OSCC cells was determined by FACS. **P<0.01 compared to control.

promoter methylation of RelA. According to Mukherjee et al. SETD6 can positively regulate p65 in bladder cancer (Mukherjee et al., 2017). In contrast, our data showed that SETD6 knockdown upregulated the expression of p65. A large part of p65 transferred into the nucleus of cells after phosphorylation, and this phenomenon can lead to the inhibition of methylation (O'Neill et al., 2014). Thereby, this discrepancy might due to the protein structure.

Frankly speaking, there are some shortcomings in this research: some rescue experiments need be supplemented to further verify whether SETD6 siRNA can inhibit the methylation of RelA and PAK4. Thus, more investigations are needed in the future.

In conclusion, silencing of SETD6 suppressed the tumorigenesis of OSCC by inhibiting methylation of PAK4 and RelA. Therefore, SETD6 might serve as a new target for treatment of OSCC.

*Conflict of interests.* These authors declared no competing interests in this study.

## References

Bai T.L., Liu Y.B. and Li B.H. (2019). MiR-411 inhibits gastric cancer proliferation and migration through targeting SETD6. Eur. Rev. Med. Pharmacol. Sci. 23, 3344-3350.

Bai X.X., Zhang J. and Wei L. (2020). Analysis of primary oral and oropharyngeal squamous cell carcinoma in inhabitants of Beijing, China-a 10-year continuous single-center study. BMC Oral. Health 20, 208.

Chen Q., Song S., Wang Z., Shen Y., Xie L., Li J., Jiang L., Zhao H., Feng X., Zhou Y., Zhou M., Zeng X., Ji N. and Chen Q. (2021). Isorhamnetin induces the paraptotic cell death through ROS and the ERK/MAPK pathway in OSCC cells. Oral. Dis. 27, 240-250.

Dai S., Horton J.R., Wilkinson A.W., Gozani O., Zhang X. and Cheng X. (2020). An engineered variant of SETD3 methyltransferase alters target specificity from histidine to lysine methylation. J. Biol. Chem. 295, 2582-2589.

Ferrari M.G., Ganaie A.A., Shabenah A., Mansini A.P., Wang L., Murugan P., Davicioni E., Wang J., Deng Y., Hoeppner L.H., Warlick C.A., Konety B.R. and Saleem M. (2020). Identifying and treating ROBO1(-ve) /DOCK1(+ve) prostate cancer: An aggressive cancer subtype prevalent in African American patients. Prostate 80, 1045-1057.

Gilligan G.M., Panico R.L., Di Tada C., Piemonte E.D. and Brunotto M.N. (2020). Clinical and Immunohistochemical epithelial profile of non-healing chronic traumatic ulcers. Med. Oral. Patol. Oral. Cir. Bucal.

Jayaraj R., Shetty S., Kumaraswamy C., Raghul S., Gothandam K.M., Raymond G., Ravishankar R.M. and Shaw P. (2020). Clinical comments on prognostic and clinicopathological significance of PD-L1 overexpression in oral squamous cell carcinoma (OSCC). Oral. Oncol. 111, 104886.

Levkau B., Scatena M., Giachelli C.M., Ross R. and Raines E.W. (1999). Apoptosis overrides survival signals through a caspase-mediated dominant-negative NF-kappaB loop. Nat. Cell. Biol. 1, 227-233.

Levy D., Kuo A.J., Chang Y., Schaefer U., Kitson C., Cheung P., Espejo A., Zee B.M., Liu C.L., Tangsombatvisit S., Tennen R.I., Kuo A.Y., Tanjing S., Cheung R., Chua K.F., Utz P.J., Shi X., Prinjha R.K., Lee K., Garcia B.A., Bedford M.T., Tarakhovsky A., Cheng X. and Gozani O. (2011). Lysine methylation of the NF-kappaB subunit RelA by SETD6 couples activity of the histone methyltransferase GLP at chromatin to tonic repression of NF-kappaB signaling. Nat. Immunol. 12, 29-36.

Liu X., Zhang L., Thu P.M., Min W., Yang P., Li J., Li P. and Xu X. (2020). Sodium cantharidinate, a novel anti-pancreatic cancer agent that activates functional p53. Sci. China. Life. Sci. (in press).

Maggirwar S.B., Ramirez S., Tong N., Gelbard H.A. and Dewhurst S. (2000). Functional interplay between nuclear factor-kappaB and c-Jun integrated by coactivator p300 determines the survival of nerve growth factor-dependent PC12 cells. J. Neurochem. 74, 527-539.

Martin-Morales L., Feldman M., Vershinin Z., Garre P., Caldes T. and Levy D. (2017). SETD6 dominant negative mutation in familial colorectal cancer type X. Hum. Mol. Genet. 26, 4481-4493.

Mukherjee N., Cardenas E., Bedolla R. and Ghosh R. (2017). SETD6 regulates NF-kappaB signaling in urothelial cell survival: Implications for bladder cancer. Oncotarget 8, 15114-15125.

Nakamichi E., Sakakura H., Mii S., Yamamoto N., Hibi H., Asai M. and Takahashi M. (2021). Detection of serum/salivary exosomal Alix in patients with oral squamous cell carcinoma. Oral. Dis. 27, 439-447.

O'Neill D.J., Williamson S.C., Alkharaif D., Monteiro I.C., Goudreault M., Gaughan L., Robson C.N., Gingras A.C. and Binda O. (2014). SETD6 controls the expression of estrogen-responsive genes and proliferation of breast carcinoma cells. Epigenetics 9, 942-950.

Oliveira Alves M.G., da Silva Miguel N., Ferreira C.C.P., Alvarenga E.R., Tonon B.M., de Barros P.P., Carta C.F.L., Paschoal M.B.N., de Sales Chagas J.F., Bandeira C.M., Nunes F.D. and Almeida J.D. (2020). Expression of DNA repair genes in oral squamous cell carcinoma using reverse transcription-quantitative polymerase chain reaction. Oral. Surg. Oral Med. Oral. Pathol. Oral. Radiol. 130, 298-308.

Sowmya S.V., Rao R.S. and Prasad K. (2020). Development of clinico-histopathological predictive model for the assessment of metastatic risk of oral squamous cell carcinoma. J. Carcinog. 19, 2.

Tang Z., Li C., Kang B., Gao G., Li C. and Zhang Z. (2017). GEPIA: a web server for cancer and normal gene expression profiling and interactive analyses. Nucleic. Acids. Res. 45, W98-W102.

Vershinin Z., Feldman M., Chen A. and Levy D. (2016). PAK4 methylation by SETD6 promotes the activation of the Wnt/beta-catenin pathway. J. Biol. Chem. 291, 6786-6795.

Vershinin Z., Feldman M. and Levy D. (2020). PAK4 methylation by the methyltransferase SETD6 attenuates cell adhesion. Sci. Rep. 10, 17068.

Walter C.E.J., Durairajan S., Periyandavan K., Doss G.P., Davis G.D.J., Vasanthi A.H.R., Johnson T. and Zayed H. (2020). Bladder neoplasms and NF-kappaB: an unfathomed association. Expert. Rev. Mol. Diagn. 20, 497-508.

Wong I.Y.H., Lam K.O., Chan W., Wong C., So T.H., Chan K.K., Choi C.W., Law T.T., Chiu K., Chan F.S.Y., Kwong D.L.W. and Law S. (2020). Real-world scenario: CROSS regimen as preoperative therapy for oesophageal cquamous cell carcinoma. J. Gastrointest. Surg. 24, 1937-1947.

Yao R., Wang Y., Han D., Ma Y., Ma M., Zhao Y., Tan J., Lu J., Xu G. and Li X. (2018). Lysines 207 and 325 methylation of WDR5 catalyzed by SETD6 promotes breast cancer cell proliferation and

migration. Oncol. Rep. 40, 3069-3077.

Zhang C., Su C., Song Q., Dong F., Yu S. and Huo J. (2018). LncRNA PICART1 suppressed non-small cell lung cancer cells proliferation and invasion by targeting AKT1 signaling pathway. Am. J. Transl. Res. 10, 4193-4201.

Zhang Y., Yan L., Yao W., Chen K., Xu H. and Ye Z. (2019). Integrated analysis of genetic abnormalities of the histone lysine methyltransferases in prostate cancer. Med. Sci. Monit. 25, 193-239.

Zhang Q., Chen S., Yang M., Wang C., Ouyang Y., Chen X., Bai J., Hu Y., Song M. and Zhang S. (2021). Forkhead promotes EMT and chemoresistance by upregulating lncRNA CYTOR in oral squamous cell carcinoma. Cancer. Lett. 503, 43-53.

Zhou S., Zhu Y., Li Z., Zhu Y., He Z. and Zhang C. (2021). Exosome-derived long non-coding RNA ADAMTS9-AS2 suppresses progression of oral submucous fibrosis via AKT signalling pathway. J. Cell. Mol. Med. 25, 2262-2273.

Accepted March 12, 2021